Journal of Engineering Science and Technology
Vol. 15, No. 2 (2020) 1384 - 1398

NUMERICAL ASSESSMENT ON FLOATING STABILITY LIMITS FOR STATIC VEHICLE UNDER PARTIAL SUBMERGENCE

EBRAHIM H. H. AL-QADAMI[1,] *, ZAHIRANIZA MUSTAFFA[1], ABDURRASHEED S. ABDURRASHEED[1], KHAMARUZAMAN W. YUSOF[1], SYED M. H. SHAH[1], M. A. MALEK[2], AMINUDDIN A. GHANI[3]

[1]Department of Civil and Environmental Engineering, Universiti Teknologi PETRONAS, Bandar Seri Iskandar, 32610, Perak, Malaysia
[2]Institute of Sustainable Energy (ISE),, Universiti Tenaga Nasional, Selangor, 43000, Malaysia
[3]River Engineering and Urban Drainage Research Center Universiti Sains Malaysia, Pulau Pinang, 11800 , Malaysia
*Corresponding Author: ialgodami@gmail.com

Abstract

Large debris including vehicles when swept by floods could threat people's life and damage properties. Concerning vehicles in floodwaters, their stability remains a challenge to the research world, particularly the buoyancy depth and the parameters affecting them to float. Therefore, a detailed investigation of the forces and mechanisms leading to floating instability mode is of utmost importance. Herein feasibility of conducting a numerical assessment to define floating instability limits of static partially submerged flooded car has been conversed and validated. A simple scaled-down car model was used with dimensions of 14.2 cm length, 5.2 cm width, and 4.5 cm height. The model was placed inside a closed box with dimensions of 35 cm length, 18.5 cm width, 5.5 cm height and with six degrees of freedom toll under the given hydrodynamic characteristics, velocity and water depth for inlet, 0 pressure with 0 fluid fraction for free top, walls for bottom and sides. The results showed that the car model started to float when the flood depth inside the box reached 1.275 cm. Further, the said approaches showed good agreement with the overall error of < 2%. The outcomes of this study can be used to assess any car models in terms of floating instability mode without the need to conduct laboratory experiments.

Keywords: Buoyancy force, Flash flood, Floating depth, Flow-3D, Numerical simulation, Vehicle stability.

1. Introduction

The probability of flash floods occurrence has increased due to climate change caused by global warming [1-3]. In 2014, a total of 324 natural disasters were reported around the world which affected 141 million people. Among the natural disasters, hydrological disaster events (floods, landslides and waves action) took a percentage of 47.2% [4]. From 1975 to 2001, a total of 1816 flood events have been reported which include flash floods and stream floods where 175,000 humans were died due to these events around the globe [5].

The danger of flash floods become significant and more harmful to people and properties [2]. In this context, vehicles recognized as one of the most dangerous factors that lead to injuries and death among the people in urban areas floods [6]. In Netherlands, the death related to drowning in vehicles during floods is about 33% and 25% as a pedestrian [7]. During the period of 1950-2004, the total death related to vehicle is about 216 people in Texas during flood roadways [8]. On 16th August 2004, Boscastle town in the UK experienced heavy rainfall event which resulted in extreme flash flood. The UK Environmental Agency reported that millions of pounds of damages were made, and huge agricultural lands were lost during this event. Nearly 116 vehicles were swept away and some of the large debris including vehicles were stacked under small bridge blocking the water stream, that eventually bridge was collapsed. Further, some of these vehicles flashed out straight to the harbor with no barriers to prevent them. [9].

Several studies have been carried out since 1967 to investigate the stability limits of flooded vehicles. An experimental study has been conducted to study the stationary vehicle stability of Ford Falcon car model with a scale of 1:25. The model was tested with flow direction facing the side end. Horizontal (F_H) and vertical (F_V) forces were measured by measuring the force on the fine threads, which restrained the model in both directions horizontally and vertically. A total of 46 combinations of flow depth and velocity were applied ranging from 0.11 to 0.57 m depth and 0.48 to 3.09 ms^{-1} velocity. It was found that the floating stability occurred at the rear part of the car at water depth of 0.57 m. After assessing the vertical and horizontal forces, the friction coefficient (μ) that leads to sliding instability was defined as 0.3 [10]. Later in 1973 laboratory test was carried out using a Morris Mini car model with a scale of 1:16 exposed to flood flow with respect to its length in a 1 m wide hydraulic flume. Two main models of resistance were considered including front wheels locked, and rear wheels locked. The results showed that the stability was a bit higher for the front wheel locked mode than for rear-wheel locked mode. This was because of the engine weight on the front side of the car [11]. Afterward theoretical study has been done to investigate stability of both vehicles and people in floodwaters. Four types of cars were used in this study including three small sizes, i.e, Suzuki Swift, Ford Laser, and Toyota Corolla, and one large size car which is Ford LTD. The flow depth ranged from 0.025 m to 0.375 m and at each flow depth vertical forces were evaluated at both axles front and rear. Horizontal forces were evaluated by determining the drag force acting on the submerged part of the vehicle, while the vertical depth was assessed by determining the weight distribution and center of buoyancy based on the manufacturer specifications [12]. The stability threshold can be expressed as:

$$U = \left[\frac{2\mu F_v}{\rho C_D A_D} \right]^{0.5} \tag{1}$$

where, U is the threshold velocity, μ is the friction coefficient, F_v is the vertical force, ρ is the water density, C_D is the drag coefficient and A_D is the submerged car area projected normally to the flood direction.

During the period between 1993 to 2010, no published research was conducted in the field of flooded vehicle stability [13]. By 2010, Teo [14] conducted experimental study to investigate the vehicles' hydraulic behaviors in urban flash floods. Experimental tests carried out inside two hydraulic flumes with different widths including 1.2 m and 0.3 m to study the effects of the width on the hydrodynamic forces exerted by the flow on the vehicles body. Three car models were used, namely BMW M5, Mini Cooper, and Mitsubishi Pajero with two different scales of 1:43 and 1:18. This study concluded that, the flooded vehicles threshold velocity under partially submerged condition decreases with increase of the flow depth. While the threshold velocity increases with increase in flow depth under fully submerged condition.

By 2013 another experimental approach was undertaken on two cars models including, Audi Q7 and Honda Accord with two scales 1:14 and 1:24. Experimental investigations were carried out inside 1.2 m wide and 60 m length laboratory hydraulic flume. Three flow orientations were taken into consideration during this study which are: 0º (car front end face flow), 180º (rear end face flow) and 90º (flow perpendicular the car length) and sets of flow depth and velocity were applied. The results showed that there is no high difference between incipient velocity for both angles of orientations of 0º and 180º, because the car submerged area projected normally to the flow direction was almost the same. The friction coefficients were measured in both direction and the values proposed were: 0.75 (flow perpendicular with car length) and 0.25 (flow parallel with car length) [15].

In 2017, an extensive experimental study with a new methodology was proposed by Martínez-Gomariz et al. [16] to investigate vehicles instability in floodwaters. 12 car models with different scales were chosen. Experiments were carried out inside 0.6 m wide and 20 m length laboratory hydraulic flume with different combinations of water depths and velocities. The friction coefficient was measured for different models and the values ranged between 0.52 and 0.62. Buoyancy depth was measured separately in small box 38.9 x 18.9 cm^2 plan area, the box filled with water till there are no connection between the tires and ground [16]. The buoyancy depth can be expressed as:

$$h_b = \left[\frac{M_c}{\rho_f l_c b_c} \right] + GC \tag{2}$$

where, h_b is the buoyancy depth, M_c is the car mass, ρ_f is the water density l_c and b_c are the car length and car width respectively, and GC is the ground clearance. Stability coefficient (SC) has been developed by Martinez-Gomariz et al. [16] based on three factors including, ground clearance GC, car plan area PA and car mass Mc, this coefficient can be written as:

$$SC = \frac{M_c GC}{PA} \tag{3}$$

Next, the modified stability coefficient ($SCmod$) was introduced related to the friction coefficient which can be expressed as:

$$SC\,\mathrm{mod} = \frac{M_c GC}{PA}\mu \tag{4}$$

The range of the modified coefficient of stability for chosen models ranged between 10.3 kg/m to 50.3 kg/m. Finally, velocity×depth stability equation was proposed which can be written as:

$$v.y = 0.0158SC\,\mathrm{mod} + 0.32 \tag{5}$$

Recently another experimental investigation had been conducted by Shah et al. [17] at the hydraulic laboratory, Universiti Teknologi PETRONAS (UTP), Malaysia using a Volkswagen Scirocco R car model with the scaled model of (1:24) to investigate stationary flooded vehicle stability. Different car model orientations with respect to flow direction were tested on flat road surface and the rear wheels were locked. The results showed that sliding instability mode occurs when the flow velocity is high and flow depth is low, while the floating instability mode occurs when the velocity is near to zero and flow depth is high. Furthermore, depth * velocity ($D \times V$) factor was obtained for orientation of 0^o (front end face flow direction) and 360^o (rear end face flow direction) to be 0.0168 m^2/s, while it was about 0.0144 m^2/s for 90^o (side part face flow direction) model orientation for scaled model [17].

To the author's best of knowledge, no prior research has been undertaken to assess the vehicles floating instability using numerical simulation with six degree of freedom function. In the present study, computational fluid dynamics (*CFD*) was used to investigate floating instability mode of flooded vehicles. Buoyancy and gravity forces were extracted at each time step. Moreover, water depth was recorded with respect to model center of mass and buoyancy force at each time step. The proposed framework herewith can be used to assess floating instability of any car models with no need to carry out experimental tests.

2. Mode of Instability and Hydrodynamic Forces

In general, there are three forms of vehicle instability during flood events namely: buoyancy or floating, sliding or friction and toppling, as shown in Fig. 1. Floating instability mode occurs when the upward forces exerted by flow under the vehicle is more than the vehicle weight, and this case of instability is commonly occurring at high flow depth and low velocity. While sliding instability occurs when the horizontal forces exerted by the flow exceeds friction force between tires and ground, which depends on total vehicle mass, buoyancy force, and the friction coefficient. Toppling mode of instability appears to be restricted to vehicles which are already sliding or floating [18]. Herein, sliding and toppling forms of instability have been excluded from future consideration.

As the floodwater flows around a parked car on the road or in the parking lots, the flow commonly exerts three hydrodynamic forces on the car, including buoyancy force (F_B), drag force (F_D) and lift force (F_L). The frictional force (F_R) between the tires and ground surface that resist the vehicle sliding movement will be produced with assumption that all car wheels are locked against any movements. The additional force generated on the flooded vehicle called gravitational force (F_G), which represented the submerged weight of the vehicle. Therefore, these

forces control the stability of a flooded vehicle as shown in Fig. 2 [13, 19]. It can be noticed that the forces acting on a flooded vehicle are almost similar to those acting on a sediment particle resting on the riverbed. However, the shape of the vehicle needs to be determined and defined before assessing the forces in detail. Vehicle shape can be characterized by the following parameters: length l_c, width b_c, height h_c and mass M_c. The volume can be written as $V_c = l_c * b_c * h_c$, and the density is $\rho_c = M_c/V_c$.

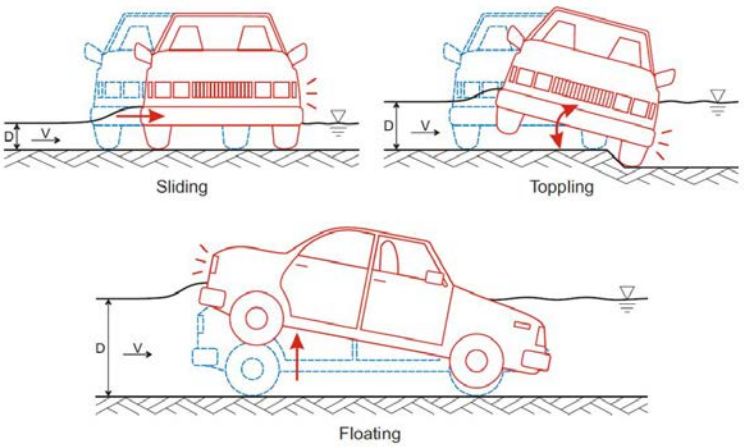

Fig. 1. Flooded vehicles typical modes of instability adopted and modified from [19].

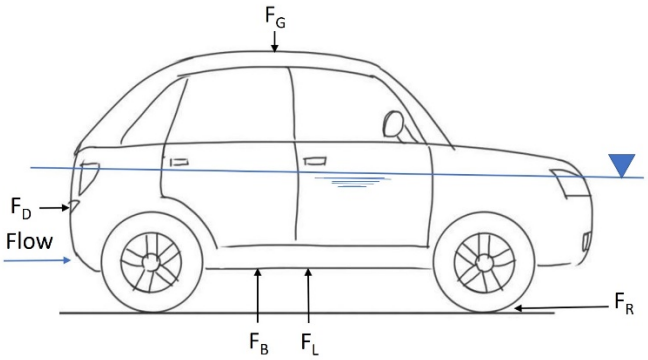

Fig. 2. Hydrodynamic forces acting on a static car adopted and modified from [13].

2.1. Drag force F_D

The drag force exerted by floodwater acting on a side of the vehicle is given in the flowing general form [20]:

$$F_D = 0.5\rho C_d A_d v^2 \quad (6)$$

where ρ is water density, A_d is the area projected normal to the incoming flow, v is flow velocity and C_d is the drag coefficient, which depends on the flow pattern and the vehicle shape.

2.2. Buoyancy force F_B

For static vehicles, the vertical pushing force, which is composed of both buoyancy and lift forces, when exceeds the vehicle weight causes floating instability. However, the buoyancy force alone can be expressed as:

$$F_B = \rho g V \tag{7}$$

where V is the vehicle submerged volume. In the recent studies [21, 22] buoyancy force alone has been taken into account for assessing floating instability mode, whereas the effects of lift force have been neglected, with the assumption that the flow velocity is small. However, in case of high flow velocity lift force alone can be taken into consideration while buoyancy force can be neglected [16].

2.3. Lift force F_L

This force can be described as a force that acts on the bottom of the vehicle in high flow velocity, and it can be expressed as:

$$F_L = 0.5\rho C_L A_L v^2 \tag{8}$$

where C_L is the lift coefficient and A_L is the affected area by the lift force. In this study the model will be simulated under subcritical flow conditions, therefore only the effect of buoyancy force will be taken into consideration for estimation of floating instability mode [20, 21].

2.4. Friction force F_R

The force exerted between tires and the ground surface against sliding is called frictional force, and it can be expressed by the following equation:

$$F_R = \mu F_N \tag{9}$$

where F_N is the magnitude of the normal reaction force from the ground surface and it can be written in a general form as $F_N = F_g - (F_L + F_B)$, and μ is the friction coefficient between tire and wet ground surface. Coefficient of friction is a material property and can be defined as a friction force which occurs between two bodies when neither the objects is moving.

3. Theory and Governing Equations

Recently, the numerical solution has become popular and common tool to solve complicated problems that cannot be done in the lab or it is expensive in terms of materials and equipment. In this study, the computational fluid dynamic (*CFD*) that uses fluid equation of motion to solve the non-linear, transient, second-order differential equations which describe the motion of the fluid was attempted. The governing equations selected to solve current simulation are continuity Eq. (10) and Reynolds-averaged Navier-Stokes Eq. (11).

$$U = \frac{\partial \rho}{\partial t} + \Delta.(\rho v) = 0 \tag{10}$$

$$\rho \frac{Dv}{Dt} = \rho g - \Delta P + \mu \Delta^2 .v \tag{11}$$

Basically, to start a numerical simulation of any problem, grid or mesh must be generated. The cells associated with each other by the nodes where the unknown parameters such as (flow velocity, flow depth, pressure, etc) are stored.

In Flow-3D, rectangular mesh for *2D* and hexahedral mesh for *3D* are available to define the grid system for numerical solution. Rectangular mesh or structured mesh is easy to construct because it is in a regular shape. Also, regular mesh gives more accurate results and helps to stabilize the numerical simulation. While unstructured mesh is not easy to generate but it is more accurate for meshing complicated domain. Each cell has its own unique call number and it is defined by three numbers *i*, *j* and *k* in *x*, *y* and *z* directions. Different modes can be run in Flow-3D, for example, compressible fluid, incompressible fluid, one fluid model, two-fluid model and free surface flow for incompressible one fluid mode. Free surface simulation mode requires accurate definition of the boundary condition of the surface that faces the air because the volume occupied by the air is replaced with an empty space, void of mass, represented by uniform pressure and temperature only.

4. Materials and Methods

In this paper, commercialized code computational fluid dynamics (*CFD*) was used for numerical simulation purpose. Flow-3D which utilizes finite volume method (*FVM*) to solve mass, continuity and momentum conservation equations was selected to simulate this case. One fluid with free surface flow was chosen and (k-ε) equations were selected to solve turbulent flow. In Flow-3D each cell has water fraction (*F*) ranged between 0 and 1 (where 1 represents cells that are full of water while 0 for cells that are full of air. *F* values less than 1 and more than 0 represent the free surface between air and water as shown in Fig. 3.

Fractional Area Volume Obstacle Representation (*FAVOR*) method was used to define the surface between the geometry body and water. The final geometry send for simulation process depends on the cells size and *FAVOR* technology can show the final geometry before starting the simulation. Hexahedral mesh blocks were defined for this 3D simulation and the total number of mesh blocks were 5,856,543 cells. A simple barrier was created and placed around the car model to reduce the turbulence of the flow due to the inlet velocity and to replicate the same experimental setups which have been done by [16]. Figures 4 and 5 show the mesh and the geometry after applying *FAVOR* solver, respectively.

A scaled down car model was created using Solidworks for this case of simulation and the 3D model was converted to *STL* format before inserting it into Flow-3D software. Car model characteristics and dimensions are presented in Fig. 5 and Table 1.

The car dimensions simply show the application of the proposed methodology /framework. This then allows the framework to be applicable to any other car models with any scale ratios to be simulated the same way.

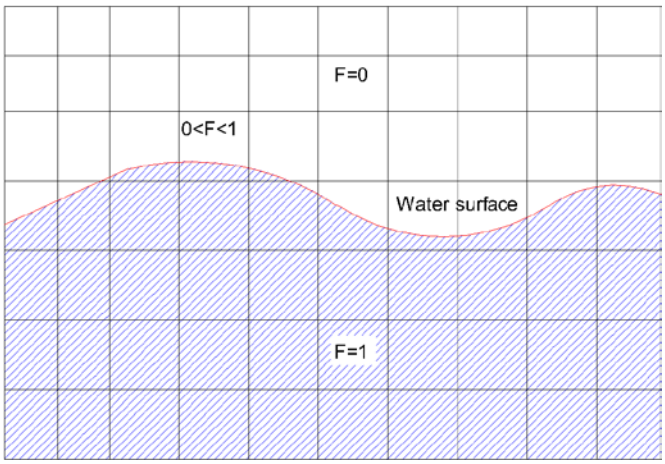

Fig. 3. Empty and full cells water volume fraction (F) adopted and modified from [23].

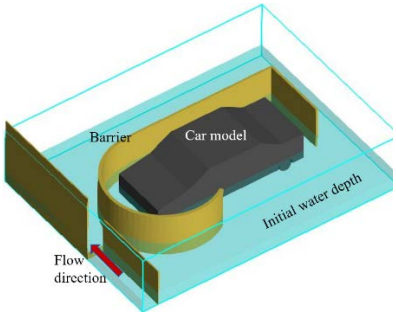

Fig. 4. Meshing and vehicle geometry inside Flow-3D.

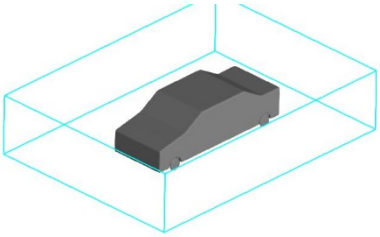

Fig. 5. Meshing and geometry after applying FAVOR solver inside Flow-3D.

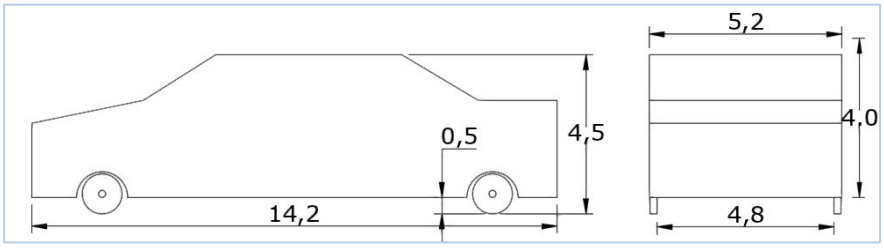

Fig. 5. Car model dimensions (cm).

Table 1. Car model dimensions and characteristics.

Length (cm)	Width (cm)	Height (cm)	GC (cm)	Density (kg/m^3)	Weight (N)	Volume (cm^3)
14.2	5.2	4.5	0.5	260	0.59	232.5

Upstream boundary condition was defined using velocity and flow depth, while downstream, channel bed and both sides were defined as walls. However, the top surface was defined as a free surface with 0 pressure and 0 fluid fraction as shown in Fig. 6. Two history probes were located in the simulation setting. The first probe was located inside the box to measure water depth as well as velocities in the *x*, *y* and *z* directions. The second probe was connected with the vehicle to record its moving. The buoyancy depth was taken from probe no.1 at the time where the car start moving in *Z* direction.

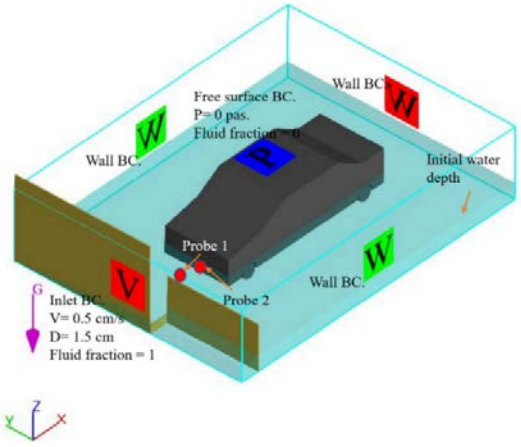

Fig. 6. Boundaries conditions settings.

5. Results and Discussion

Floating instability mode occurs when the upward forces (F_B) exerted by the flood exceed the weight of the vehicle (F_G). Upward forces can be divided into two main components which include buoyancy force and lift force. In case of low flow velocity lift force can be neglected [15]. In this paper, buoyancy force alone has been considered to investigate the floating instability mode. Figure 7 shows the relationship between the buoyancy force exerted by the water body and the gravitational force exerted by the vehicle weight. At time t=0 s the upward force (buoyancy force) was equal to 0.53934 *N*. This was due to the initial water depth inside the box. The buoyancy force at t=0 was less than the weight of the car model (i.e. no buoyancy instability). After 5 s buoyancy force (F_B) increased to reach 0.59274 *N* due to the increasing of the water depth inside the box as shown in Fig. 8. At that moment F_B was equal to the car model weight (i.e. starting of floating instability). It can be noticed that the floating instability mode was occurred exactly when the buoyancy force exerted by the water was equal to the car model weight at dry condition as expected.

Figure 9 shows the behavior of the car model center of mass in the *Z* direction with the water depth variation. The center of mass was at its original position until the water depth reached to 1.275 cm then the car model started to float. Figure 10 shows the car model center of mass behavior with the variation of the buoyancy depth where the car model starts to move when the buoyancy force is greater than the vehicle weight. It was clear that the car ground clearance and the plane area have big effects on the buoyancy depth and buoyancy force. A car model with high ground clearance and less plane area required more water depth to float.

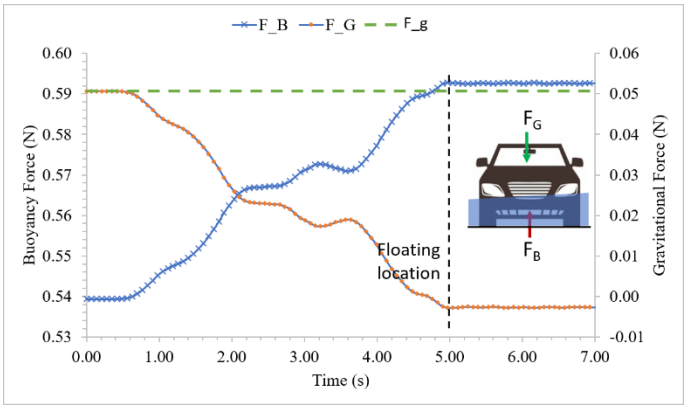

Fig. 7. Buoyancy force variations with gravitational force at different times of simulation.

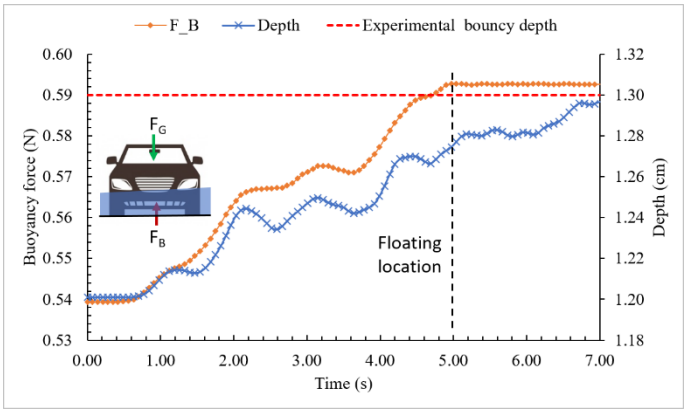

Fig. 8. Buoyancy force variations with water depth at different times of simulation.

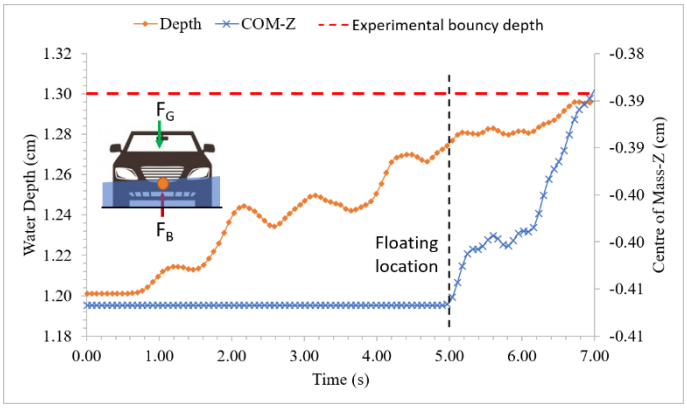

Fig. 9. Center of mass (COM) in Z direction variations with water depth at different times of simulation.

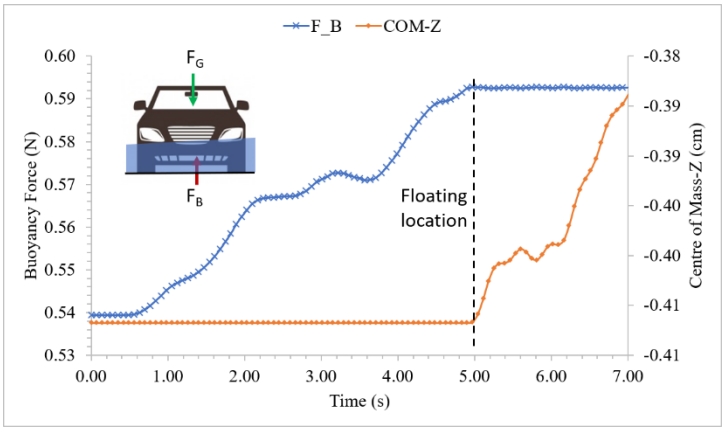

Fig. 10. Center of mass (COM) in Z direction variations with buoyancy force at different times of simulation.

To ensure that the flow velocity in the ±*x* and ±*y* directions around the car model is at the minimal values to produce the same conditions of the previous experimental tests, barrier around the vehicle was placed. From the history probe near the car model the velocity in -*x* and -*y* direction, as well as the Froude number were calculated at each time step. Figure 11 shows the variation of flow velocity and Froude number, where the maximum *x* velocity was 0.08 cm/s, maximum y velocity was 0.04 cm/s and Froude number was less than 0.1.

Figure 12 shows the pressure distribution in the bottom part of the vehicle where the pressure distributed equally on the plan area of the car, while around the tires it seems greater than the plan area due to the difference in water depth. The flow depth and pressure distribution in 3-D view are shown in Fig. 13, where the buoyancy depth found to be 1.275 cm which is more than the ground clearance by 0.775 cm.

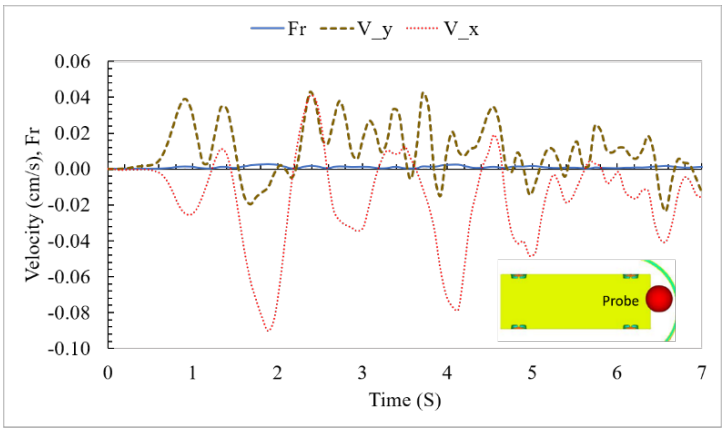

Fig. 11. *x* velocity, *y* velocity and Froude number variations with time at different times of simulation.

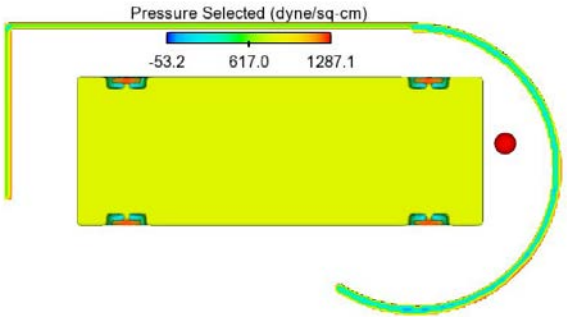

Fig. 12. Pressure distribution at the bottom plan of the car at time *t*= 7 s.

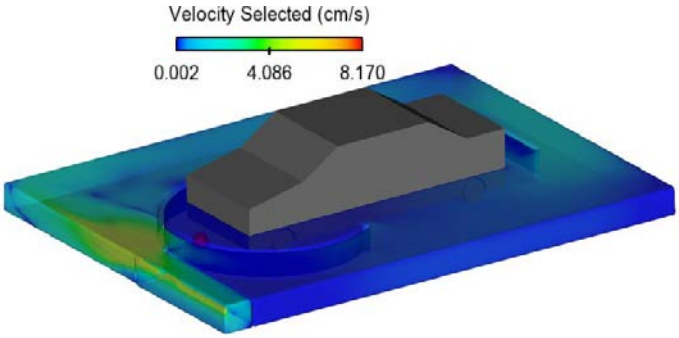

Fig. 13. Flow velocity and depth around the car model at time *t*= 7 s.

Buoyancy depth h_b was validated based on the previous study which has been done by Martínez-Gomariz et al. [16], where the buoyancy depth can be calculated by:

$$h_b = \left[\frac{M_c}{\rho_f l_c b_c}\right] + GC \tag{12}$$

where, *Mc* is the car mass = 59 gm, ρ is the water density = 1000 kg/m^3, l_c & b_c are the length and width of the car which are 14.2 cm and 5.2 cm respectively and *GC* is the ground clearance 0.5 cm. From Eq. (12), buoyancy depth is equal to 1.3 cm which is close enough to the buoyancy depth from the numerical simulation. The difference between the simulation results and experimental one was 1.94% which is quite small. However, buoyancy force from numerical simulation which is 0.59274 N can be compared with the gravitational force due to the car weight, which is 0.59 N, which means good overlap between both results. Table 2 shows a summary of the results and the validation.

Table 2. Summary of results and validation.

Parameter	Martnez-Gomariz et al. 2017	Numerical simulation	Variation %
Buoyancy depth (cm)	1.30	1.275	1.94
Buoyancy force (*N*)	0.59	0.593	0.50

6. Conclusions

In this study, floating instability mode of flooded vehicle has been numerically investigated by using commercial code called FLOW-3D. Numerical simulation was conducted on a scaled down car model that has dimensions of 14.2 cm length, 5.2 cm width, 4.5 cm height, and 0.5 cm ground clearance. The results revealed that the buoyancy depth for the selected model was 1.275 cm which was 0.757 cm higher than the car ground clearance. The buoyancy depth was validated based on the results of the experimental study. An acceptable difference of 1.94% between both results was observed. Moreover, it was noticeable that the center of mass (*COM*) of the car model remained at its original location until the buoyancy force (F_B) exceeded the car weight at the dry condition (*Fg*). Then, the *COM* started to move resulting in floating instability mode. Meanwhile, car weight, ground clearance, flow velocity, and car plane area were the most critical parameters effecting floating instability of flooded vehicles. This study, therefore, can be considered as an alternative for laboratory experiments. Future study can be conducted to investigate sliding instability mode of flooded vehicles using FLOW-3D software and six degree of freedom function.

Acknowledgment

The authors acknowledge Universiti Teknologi PETRONAS, Malaysia for providing the enabling environment and hydraulic laboratory equipment to be utilized for this research.

Nomenclatures

A_D	Normal projected area to the flow direction, m^2
A_L	Area affected by lift force, m^2
b_c	Vehicle width, m
C_D	Drag coefficient
C_L	Lift coefficient
F_B	Buoyancy force, N
F_D	Drag force, N
F_g	Gravitational force, N
F_L	Lift force, N
F_N	Normal force, N
F_R	Friction force, N
F_V	Vertical forces, N
g	Gravity, m/s^2
GC	Ground clearance, m
h_b	Buoyancy depth, m
l_c	Vehicle length, m
M_c	Vehicle mass, kg
P	Pressure, Pa
PA	Plane area, m^2
SC	Stability coefficient
SC_{mod}	Modified stability coefficient
t	Time, *s*

U	Threshold velocity, m/s
v	Flow velocity, m/s
V	Submerged vehicle volume, m^3
y	Flow depth, m

Greek Symbols

μ	Coefficient of friction
ρ	Density, kg/m^3

Abbreviations

CFD	Computational Fluid Dynamics
F	Water Fraction
FAVOR	Fractional Area Volume Obstacle Representation
FVM	Finite Volume Method

References

1. McMichael, A.J.; Woodruff, R.E.; and Hales, S. (2006). Climate change and human health: present and future risks. *The Lancet*, 367(9513), 859-869.
2. Andersen, T.K.; and Marshall Shepherd, J. (2013). Floods in a changing climate. *Geography Compass*, 7(2), 95-115.
3. Thistlethwaite, J.; Minano, A.; Blake, J. A.; Henstra, D.; and Scott, D. (2018). Application of re/insurance models to estimate increases in flood risk due to climate change. *Geoenvironmental Disasters*, 5(1), 1-9.
4. Guha-Sapir, D.; Vos, F.; Below, R.; and Ponserre, S. (2011). Annual disaster statistical review 2010. *Centre for Research on the Epidemiology of Disasters*. Université Catholique de Louvain, Brussels, Belgium.
5. Jonkman, S.N.; and Penning Rowsell, E. (2008). Human Instability in Flood Flows 1. *JAWRA Journal of the American Water Resources Association*, 44(5), 1208-1218
6. Anderson, W.A.; Ressler, E.; and Kennedy, P.J. (2007). Handbook of disaster research (Vol. 643). H. Rodrguez, E. L. Quarantelli, and R. R. Dynes (Eds.). *New York: Springer*.
7. Jonkman, S.N.; and Kelman, I. (2005). An analysis of the causes and circumstances of flood disaster deaths. *Disasters*, 29(1), 75-97.
8. Maples, L.Z.; and Tiefenbacher, J.P. (2009). Landscape, development, technology and drivers: The geography of drownings associated with automobiles in Texas floods, 19502004. *Applied geography*, 29(2), 224-234.
9. Xia, J.; Falconer, R.A.; Lin, B.; and Tan, G. (2011). Numerical assessment of flood hazard risk to people and vehicles in flash floods. *Environmental Modelling and Software*, 26(8), 987-998.
10. Bonham, A.J.; and Hattersley, R.T. (1967). Low level causeways. University of New South Wales, *Water Research Laboratory*, Technical Report No. 100.
11. Gordon, A.D.; and Stone, P.B. (1973). Car Stability on Road Causeways. WRL Technical Report No. 73/12. 5p + Appendices. Institution.

12. Keller, R.J. and Mitsch, B. (1993). Safety Aspects of the Design of Roadways as Floodways, Research Report No. 69, Urban Water Research Association of Australia. Melbourne.
13. Shah, S.M.H.; Mustaffa, Z.; Martinez-Gomariz, E.; Kim, D.K.; and Yusof, K.W. (2019). Criterion of vehicle instability in floodwaters: past, present and future. *International Journal of River Basin Management*, 1- 23.
14. Teo, F.Y. (2010). Study ofthe hydrodynamic processes ofrivers and flood-plains with obstructions. Thesis (PhD). Available from: https://orca.cf.ac.uk/54161/1/U517543.pdf.
15. Xia, J.; Falconer, R.A.; Xiao, X.; and Wang, Y. (2014). Criterion of vehicle stability in floodwaters based on theoretical and experimental studies. *Natural hazards*, 70(2), 1619-1630.
16. Martnez-Gomariz, E.; Gmez, M.; Russo, B.; and Djordjevic, S. (2017). A new experiments-based methodology to define the stability threshold for any vehicle exposed to flooding. *Urban Water Journal*, 14(9), 930-939.
17. Shah, S. M. H.; Mustaffa, Z.; and Yusof, K. W. (2018). Experimental studies on the threshold of vehicle instability in floodwaters. *Jurnal Teknologi*, 80(5), 25-36.
18. Cox, R.J.; Shand, T.D.; and Blacka, M.J. (2010). Australian rainfall and runoff revision project, Project 10, Appropriate safety criteria for people. Engineers Australia Water Engineering.
19. Shand, T.D.; Cox, R.J.; Blacka, M.J; and Smith, G.P. (2011). Australian Rainfall and Runoff (AR&R). Revision Project 10: Appropriate safety criteria for vehicles, (Report Number: P10/S2/020). Sydney: Water Research Laboratory, 19.
20. Chien, N.; and Wan, Z. (1999). Mechanics of sediment transport. *American Society of Civil Engineers Press*. ISBN:9780784478905
21. Shu, C.; Xia, J.; Falconer, R.; and Lin, B. (2011). Estimation of incipient velocity for partially submerged vehicles in floodwaters. *Journal of Hydraulic Research*, 49 (6), 709-717.
22. Teo, F.Y.; Xia, J.; Falconer, R.A.; and Lin, B. (2012). Experimental studies on the interaction between vehicles and floodplain flows. *International journal of river basin management*, 10(2), 149-160.
23. Abdurrasheed, S. A.; Yusof, K.W.; Al-Qadami, E.H.H.; Takaijudin, H.; Ghani, A.A.; Muhammad, M.M.; Sholagberu, A.T.; Zainalfikry, M.K.; Osman, M.; and Patel, M.S. (2019). Modelling of flow parameters through subsurface drainage modules for application in BIOECODS. *Water*, 11(9), 18-23.